Available online at www.sciencedirect.com
SCIENCE DIRECT®
Carbohydrate Research 339 (2004) 483–491
Carbohydrate RESEARCH

Characterization and detection of lysine–arginine cross-links derived from dehydroascorbic acid

Oliver Reihl,* Markus O. Lederer and Wolfgang Schwack

Institut für Lebensmittelchemie (170), Universität Hohenheim, Garbenstr. 28, D-70593 Stuttgart, Germany

Received 29 July 2003; received in revised form 2 December 2003; accepted 6 December 2003

Abstract—Covalently cross-linked proteins are among the major modifications caused by the advanced Maillard reaction. So far, the chemical nature of these aggregates is largely unknown. L-Dehydroascorbic acid (DHA, **5**), the oxidation product of L-ascorbic acid (vitamin C), is known as a potent glycation agent. Identification is reported for the lysine–arginine cross-links N^6-[2-[(4-amino-4-carboxybutyl)amino]-5-(2-hydroxyethyl)-3,5-dihydro-4*H*-imidazol-4-ylidene]-L-lysine (**9**), N^6-[2-[(4-amino-4-carboxybutyl)amino]-5-(1,2-dihydroxyethyl)-3,5-dihydro-4*H*-imidazol-4-ylidene]-L-lysine (**11**), and N^6-[2-[(4-amino-4-carboxybutyl)amino]-5-[(1*S*,2*S*)-1,2,3-trihydroxypropyl]-3,5-dihydro-4*H*-imidazol-4-ylidene]-L-lysine (**13**). The formation pathways could be established starting from dehydroascorbic acid (**5**), the degradation products 1,3,4-trihydroxybutan-2-one (**7**, L-erythrulose), 3,4-dihydroxy-2-oxobutanal (**10**, L-threosone), and L-*threo*-pentos-2-ulose (**12**, L-xylosone) were proven as precursors of the lysine–arginine cross-links **9**, **11**, and **13**. Products **9** and **11** were synthesized starting from DHA **5**, compound N^6-[2-[(4-amino-4-carboxybutyl)amino]-5-[(1*S*,2*R*)-1,2,3-trihydroxypropyl]-3,5-dihydro-4*H*-imidazol-4-ylidene]-L-lysine (**16**) via the precursor D-*erythro*-pentos-2-ulose (**15**). The present study revealed that the modification of lysine and arginine side chains by DHA **5** is a complex process and could involve a number of reactive carbonyl species.

Keywords: Maillard reaction; Dehydroascorbic acid; Advanced glycation end product (AGE); L-Erythrulose; Cross-links

1. Introduction

The reaction between reducing carbohydrates and lysine side chains or N-terminal amino groups of proteins is known as the Maillard reaction or 'non-enzymatic browning'. This process initially leads to a rather unstable Schiff base, which rearranges to the more stable Amadori product. The Amadori compounds are slowly degraded, in complex reaction pathways via dicarbonyl intermediates, to a large number of compounds[1,2] summarized as 'advanced glycation end products' (AGEs). This overall reaction sequence proceeds in vitro, in the living organism, and in foods. A major consequence of the advanced Maillard reaction is the formation of covalently cross-linked proteins which, in long-lived tissue proteins, such as collagen and eye lens crystallins, accumulate with age. Several studies reported about the risk factor of AGEs-formation in the development of different medical complications including cataract formation,[3] retinopathy,[4] and nephropathy.[5] The formation of AGEs are also responsible for the decreased flexibility of collagen[6] and the high level of urea-insoluble proteins in human cataracts.[7] Among these, reactions leading to inter- or intramolecular protein cross-linking are of special importance for the nutritional and functional properties of various foods.[8] On the basis of various model reactions, different mechanisms for

Abbreviations: AGE, advanced glycation end product; DOGDIC **3**, N^6-{2-{[(4*S*)-4-ammonio-5-oxido-5-oxopentyl]amino}-5-[(2*S*,3*R*)-2,3,4-trihydroxybutyl]-3,5-dihydro-4*H*-imidazol-4-ylidene}-L-lysinate; GODIC **2**, N^6-(2-{[(4*S*)-4-ammonio-5-oxido-5-oxopentyl]amino}-3,5-dihydro-4*H*-imidazol-4-ylidene)-L-lysinate; MODIC **1**, N^6-(2-{[(4*S*)-4-ammonio-5-oxido-5-oxopentyl]amino}-5-methyl-3,5-dihydro-4*H*-imidazol-4-ylidene)-L-lysinate.

* Corresponding author. Tel.: +49-711-4594099; fax: +49-711-45940-96; e-mail: oreihl@uni-hohenheim.de

0008-6215/$ - see front matter © 2003 Elsevier Ltd. All rights reserved.
doi:10.1016/j.carres.2003.12.004

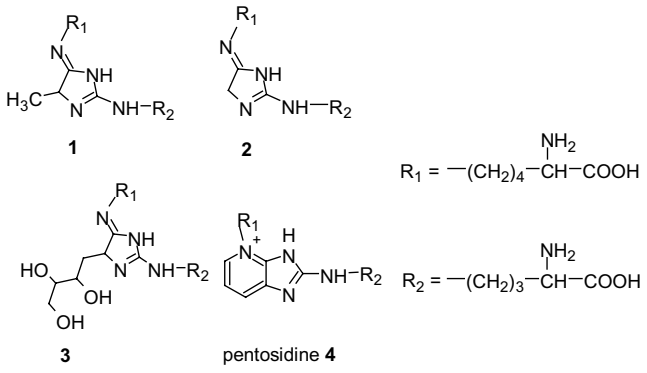

Figure 1. Structural formulas of major protein cross-links: MODIC **1**, GODIC **2**, DOGDIC **3**, and pentosidine **4**.

cross-linking of amino acid side chains in proteins have been discussed.[9–20] So far, pentosidine **4** (Fig. 1),[21] fluorophore LM-1,[22,23] crossline,[24] MOLD,[25] GOLD,[26,27] carboxymethyllysine,[28] MODIC **1**, GODIC **2** (Fig. 1), and glucosepane[29] have been detected in vivo.

L-Dehydroascorbic acid (DHA, **5**), the oxidation product of L-ascorbic acid (vitamin C), is known as a potent glycation agent. Several in vitro studies have shown that **5** is much more reactive than glucose and fructose in glycation of lens proteins,[30] thus **5** is a possible important precursor for the formation of AGEs in vivo. At that time, only a few AGEs obtained by degradation of **5** with lysine residues were established.[31,32] The major resultant products of dehydroascorbic acid (**5**) under physiological conditions were found to be L-erythrulose (**7**) and oxalate (see Scheme 1).[33] Shin and Feather[34] reported L-*threo*-pentos-2-ulose (L-xylosone, **12**) as another intermediate during the degradation of dehydroascorbic acid (**5**).

The purpose of the present study was the structural characterization of novel lysine–arginine cross-links and the elucidation of their formation pathways starting from dehydroascorbic acid (**5**, see Scheme 1). For the first time, we reported of three lysine–arginine cross-links obtained by degradation of DHA: N^6-[2-[(4-amino-4-carboxybutyl)amino]-5-(2-hydroxyethyl)-3,5-dihydro-4*H*-imidazol-4-ylidene]-L-lysine (**9**), N^6-[2-[(4-amino-4-carboxybutyl)amino]-5-(1,2-dihydroxyethyl)-3,5-dihydro-4*H*-imidazol-4-ylidene]-L-lysine (**11**), and N^6-[2-[(4-amino-4-carboxybutyl)amino]-5-[(1*S*,2*S*)-1,2,3-trihydroxypropyl]-3,5-dihydro-4*H*-imidazol-4-ylidene]-L-lysine (**13**).

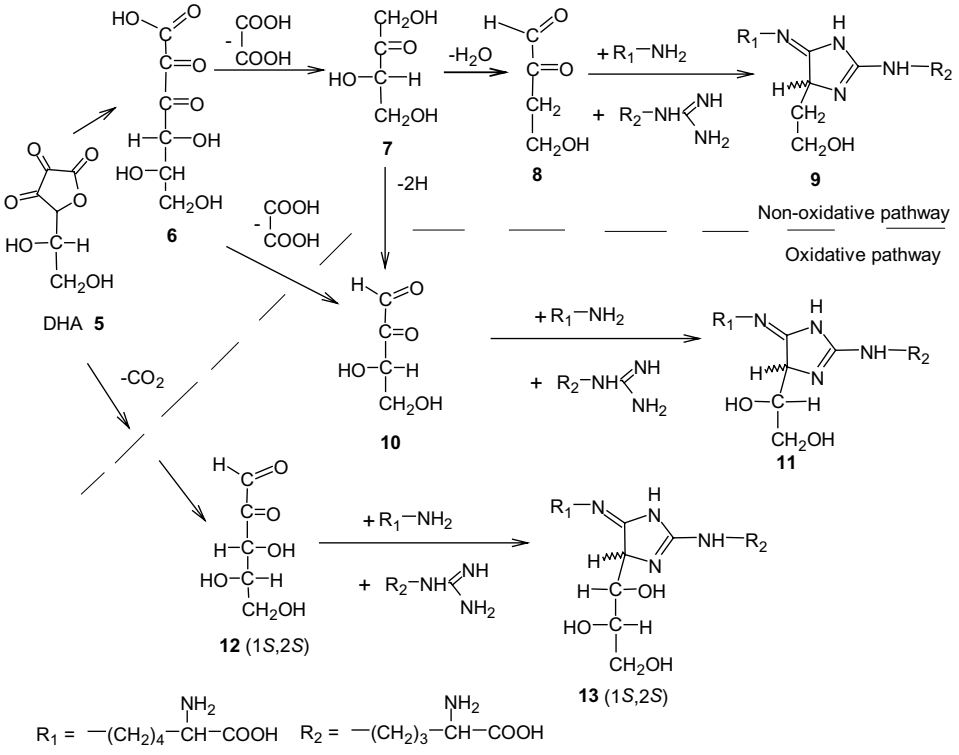

Scheme 1. Proposed mechanism for the formation of the lysine–arginine cross-links N^6-[2-[(4-amino-4-carboxybutyl)amino]-5-(2-hydroxyethyl)-3,5-dihydro-4*H*-imidazol-4-ylidene]-L-lysine (**9**), N^6-[2-[(4-amino-4-carboxybutyl)amino]-5-(1,2-dihydroxyethyl)-3,5-dihydro-4*H*-imidazol-4-ylidene]-L-lysine (**11**), and N^6-[2-[(4-amino-4-carboxybutyl)amino]-5-[(1*S*,2*S*)-1,2,3-trihydroxypropyl]-3,5-dihydro-4*H*-imidazol-4-ylidene]-L-lysine (**13**) by degradation of dehydroascorbic acid (DHA, **5**).

2. Results and discussion

2.1. Formation of the novel DHA–lysine–arginine cross-links

As previously shown,[35,36] MODIC **1**, GODIC **2**, and DOGDIC **3** (Fig. 1) are formed from the reaction of L-lysine and L-arginine with the respective dicarbonyl compounds methylglyoxal (MGO), glyoxal (GO), and 3-deoxyglucosone (3-DOG).[35,36] They belong together to the group of amino imidazolinimine cross-links. Related AGEs bearing an amino imidazolinone core structure, as well as their dehydrogenated follow-up products, have already been described.[37–40] Incubation of DHA **5** with N^{α}-*t*-Boc-L-lysine and N^{α}-*t*-Boc-L-arginine was performed in $NaHCO_3$ buffer pH 8 at 37.4 °C for 7 days. LC–(ESI)MS analysis of the crude reaction mixture show signals with $[M+H]^+$ at m/z 587 (*t*-Boc-**9**, see Fig. 2, trace A) and m/z 633 (*t*-Boc-**13**, trace C), and an additional peak with the quasimolecular ion $[M+H]^+$ at m/z 603 (*t*-Boc-**11**, trace B), that is, 16 Da higher than the $[M+H]^+$ signal of *t*-Boc-**9**. This result can only be explained by an oxidation process. Signals with $[M+H]^+$ at m/z 557 and 543, were also detected in the LC–MS chromatogram (see Fig. 2, traces D, E), the respective $[M+H]^+$ ion masses and the corresponding retention times were identical to those, reported for *t*-Boc-MODIC-**1** and *t*-Boc-GODIC-**2**.[36] Formation of these cross-links proved methylglyoxal (MGO) and glyoxal (GO) being formed during degradation of **5**. Due to the very low product amount, isolation and characterization of **13** with $[M+H]^+$ at m/z 433 was not practicable. The independent synthesis and unequivocal structural characterization of the stereoisomer **16** will be described in the next section. The protective groups were cleaved off in acidic medium (3 M HCl) and **9** and **11** with $[M+H]^+$ at m/z 387 and 403, respectively, were purified by preparative HPLC, using an ammonium formate buffer–methanol gradient. Accurate mass determination of the obtained compounds gave $[M+H]^+$ at m/z 387.2356 (**9**) and m/z 403.2305 (**11**), confirming the expected elemental composition $C_{16}H_{31}N_6O_5$ and $C_{16}H_{31}N_6O_6$, respectively. The NMR data for **9** and **11** are given in Table 1. The ^{13}C chemical shifts and connectivities definitely proved the outlined structures for N^6-[2-[(4-amino-4-carboxybutyl)amino]-5-(2-hydroxyethyl)-3,5-dihydro-4*H*-imidazol-4-ylidene]-L-lysine (**9**) and N^6-[2-[(4-amino-4-carboxybutyl)amino]-5-(1,2-dihydroxyethyl)-3,5-dihydro-4*H*-imidazol-4-ylidene]-L-lysine (**11**) in Scheme 1.

To confirm the results, D-erythrose was incubated with N^{α}-*t*-Boc-L-lysine and N^{α}-*t*-Boc-L-arginine in $NaHCO_3$ buffer pH 7.4 at 50 °C for 24 h. The LC–(ESI)MS monitored reaction showed the formation of signals with $[M+H]^+$ at m/z 587 (*t*-Boc-**9**, trace A) and m/z 603 (*t*-Boc-**11**, trace B), respectively (see Fig. 3). The retention times, UV, and mass spectra (data not shown) were identical to those, isolated from the reaction system of DHA **5**, N^{α}-*t*-Boc-L-lysine, and N^{α}-*t*-Boc-L-arginine (see Fig. 2).

Nagaraj and Monnier[32] claimed the glycation product 2-acetamindo-6-(3-(1,2-dihydroxyethyl)-2-formyl-4-hydroxymethyl-1-pyrrol) hexanoic acid as the major

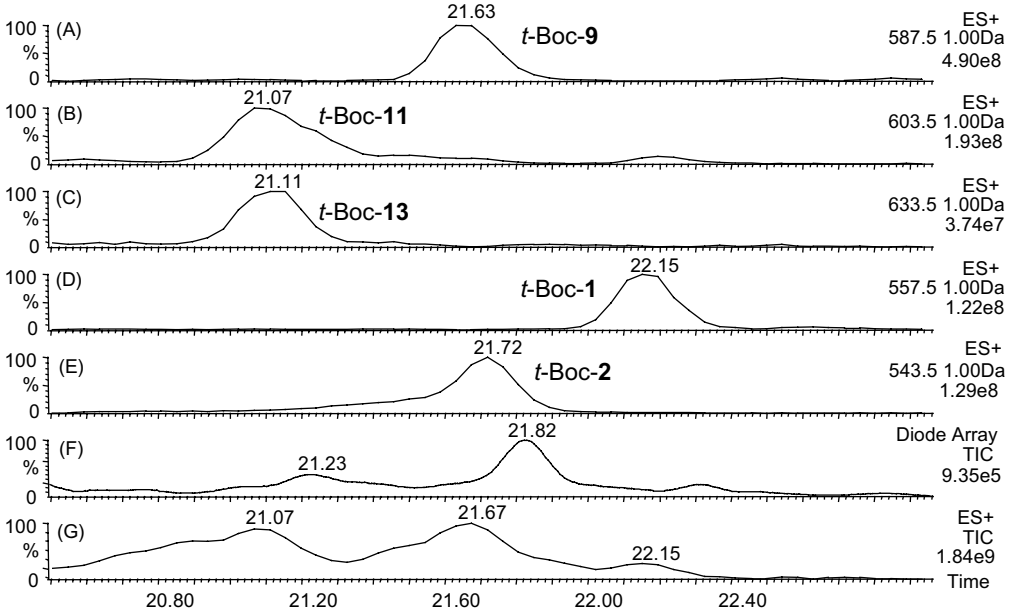

Figure 2. Chromatograms for a reaction mixture of dehydroascorbic acid (**5**), N^{α}-*t*-Boc-L-lysine, and N^{α}-*t*-Boc-L-arginine: (A–C) $[M+H]^+$ ion traces of the *t*-Boc-derivatives **9** (m/z 587), **11** (m/z 603), and **13** (m/z 633); (D, E) $[M+H]^+$ ion traces of *t*-Boc-MODIC **1** (m/z 557) and *t*-Boc-GODIC **2** (m/z 543); (F) 'TIC' of the DAD, operating from 220 to 500 nm; (G) MS–TIC recorded for the mass range m/z 200–1000.

Table 1. ^{1}H and ^{13}C NMR data of **9**, **11**, and **16a**,**b**[a] in D_2O

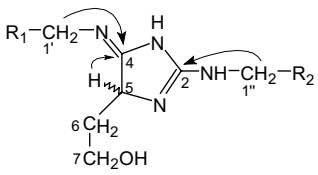

9

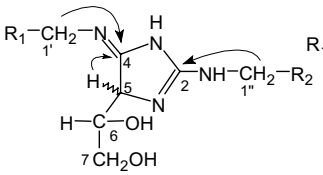

11

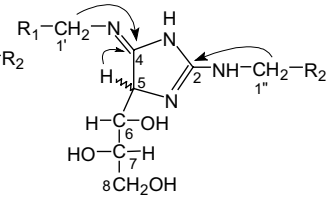

16a,b (1S,2R)

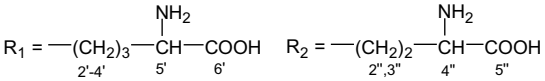

^{1}H NMR	δ (ppm)[b]			
	9	**11**	**16a**	**16b**
H-5	4.82	4.88	5.07	4.49
H-6	—	4.09	3.92	4.01
H_A-6	2.00	—	—	—
H_B-6	2.14	—	—	—
H-7	3.66	3.67	3.67	3.71
H_A-8	—	—	3.72	3.62
H_B-8	—	—	3.82	3.75
H_2-1′	3.42	3.46	3.53	3.41
H_2-2′	1.67	1.68	1.67	1.65
H_2-3′	1.42	1.41	1.42	1.42
H_2-4′	1.84	1.86	1.87	1.77
H_2-5′	3.71	3.76	3.71	3.70
H_2-1″	3.34	3.38	3.45	3.36
H_2-2″	1.72	1.71	1.65	1.72
H_2-3″	1.86	1.90	1.89	1.91
H-4″	3.75	3.75	3.76	3.74
			J (Hz)[c]	
$^{2}J_{6A,6B}$	(−)14.1	—	—	—
$^{2}J_{8A,8B}$	—	—	—[d]	—[d]
$^{3}J_{5,6}$	—	1.7	1.7	3.1
$^{3}J_{5,6A}$	6.0	—	—	—
$^{3}J_{5,6B}$	5.4	—	—	—
$^{3}J_{6,7}$	—	5.9	8.5	7.8
$^{3}J_{6A,7}$	6.2	—	—	—
$^{3}J_{6B,7}$	6.2	—	—	—
$^{3}J_{7,8A}$	—	—	—[d]	—[d]
$^{3}J_{7,8B}$	—	—	—[d]	—[d]
$^{3}J_{1',2'}$	6.8	6.8	6.5	7.5
$^{3}J_{4',5'}$	6.0	6.1	6.1	6.1
$^{3}J_{1'',2''}$	6.8	6.8	6.8	6.9
$^{3}J_{3'',4''}$	6.0	—[d]	6.2	6.4

^{13}C NMR	δ (ppm)[b]			
C-2	166.0	168.4	168.7	168.0
C-4	179.0	178.4	179.1	177.8
C-5	60.5	64.4	62.9	65.5
C-6	34.3	71.3	70.9	71.0
C-7	57.6	63.0	72.3	71.8
C-8	—	—	64.8	62.5
C-1′	43.1	43.0	43.3	43.0
C-2′	27.9	27.4	27.8	27.1
C-3′	22.0	22.0	21.9	22.0
C-4′	30.3	30.2	30.3	30.2
C-5′	55.0	55.0	55.0	54.8
C-6′	173.5	175.4	175.2	174.8
C-1″	42.0	42.0	42.6	42.5

Table 1 (*continued*)

^{13}C NMR	δ (ppm)[b]			
	9	**11**	**16a**	**16b**
C-2″	24.7	24.4	24.2	24.0
C-3″	28.0	27.7	28.0	28.0
C-4″	54.8	55.0	54.8	54.5
C-3″	173.0	174.4	174.8	174.4

[a]The arrows in the structural formulas indicate the characteristic carbon–proton long-range coupling connectivities from the gs-HMBC spectra. Hydrogen/carbon assignment has been validated by ^{1}H,^{1}H-COSY, gs-HSQC, and gs-HMBC measurements.
[b]δ (ppm), chemical shift for the indicated hydrogen/carbon.
[c]J (Hz), coupling constant between the indicated protons.
[d]No coupling constant can be determined, due to overlapping multiplets.

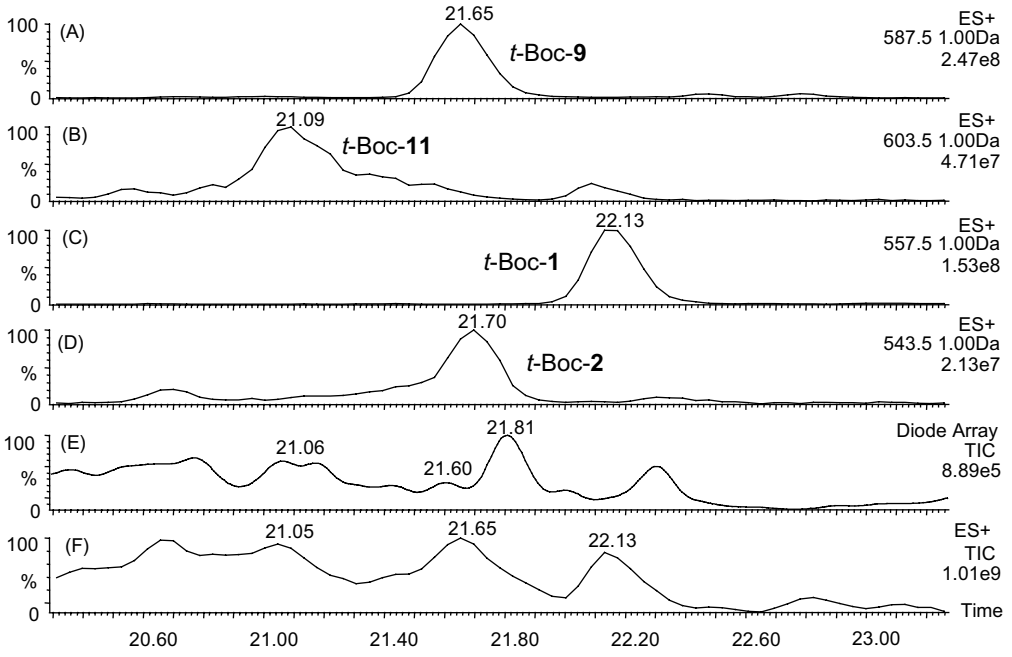

Figure 3. Chromatograms for a reaction mixture of D-erythrose, N^{α}-*t*-Boc-L-lysine, and N^{α}-*t*-Boc-L-arginine: (A, B) $[M+H]^{+}$ ion traces of the *t*-Boc-derivatives **9** (m/z 587) and **11** (m/z 603); (C, D) $[M+H]^{+}$ ion traces of *t*-Boc-MODIC **1** (m/z 557) and *t*-Boc-GODIC **2** (m/z 543); (E) 'TIC' of the DAD, operating from 220–500 nm; (F) MS–TIC recorded for the mass range m/z 200–1000.

degradation product of dehydroascorbic acid (**5**). This compound is formed by condensation of the ε-amino group of lysine with one molecule of L-threose forming the Amadori compound of L-threose and of one molecule of 4-hydroxy-2-oxobutanal (3-deoxythreosone, **8**). A recent study[33] has shown L-erythrulose (**7**) is the major degradation product of the non-oxidative degradation of **5**. The hydrolysis of **5** gave 2,3-diketogulonic acid (**6**), which is transformed to **7** and oxalate (see Scheme 1). L-Erythrulose (**7**) should be very reactive toward amino acid amino groups since **7** appears in solution to exist nearly 100% in the free carbonyl form.[33]

The non-oxidative degradation pathway of **5** predominantly produced **7** and oxalic acid, which was also confirmed by our results. The major degradation product **7** rapidly rearranged under water elimination to the α-dicarbonyl compound 4-hydroxy-2-oxobutanal (**8**) the precursor of the lysine–arginine cross-link N^{6}-[2-[(4-amino-4-carboxybutyl)amino]-5-(2-hydroxyethyl)-3,5-dihydro-4*H*-imidazol-4-ylidene]-L-lysine (**9**). The formation of GODIC **2** and MODIC **1** (see Figs. 2 and 3) could be explained by a degradation of **7** forming glyoxal and methylglyoxal, respectively.

Nishikawa et al.[41] identified 3,4-dihydroxy-2-oxobutanal (**10**, L-threosone) as an intermediate compound in the oxidative degradation process of **5**. On one hand, L-threosone (**10**) can be formed by oxidation of the C-1-alcohol group of **7**, on the other hand by a single fission reaction of the C-2–C-3 bond of **6** with the equimolar formation of oxalic acid or by two successive decarboxylation processes. Reaction of **10** with lysine and arginine residues yields the Maillard cross-link N^{6}-[2-[(4-amino-4-carboxybutyl)amino]-5-(1,2-dihydroxyethyl)-3,5-dihydro-4*H*-imidazol-4-ylidene]-L-lysine (**11**).

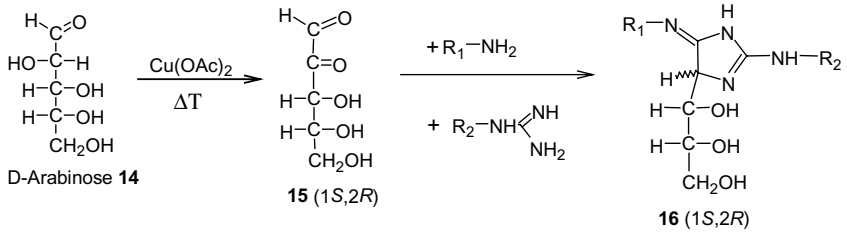

Scheme 2. Reaction pathway for the formation of **16** via the intermediate D-*erythro*-pentos-2-ulose (**15**).

Compounds **9** and **11** represent the first lysine–arginine cross-links described so far formed from tetroses (see Scheme 1).

Shin and Feather[34] reported L-*threo*-pentos-2-ulose (**12**) as an intermediate in the degradation pathway of dehydroascorbic acid (**5**). Incubation of **5** with N^{α}-*t*-Boc-L-lysine and N^{α}-*t*-Boc-L-arginine showed one peak with $[M+H]^+$ at m/z 633 (*t*-Boc-**13**, see Fig. 2, trace C). Formation of **13** requires the intermediate L-*threo*-pentos-2-ulose (**12**, see Scheme 1), a decarboxylation product of **5**. Due to very low product amounts of **13** gained by reaction of **5** with lysine and arginine, we performed the synthesis of **16**, a stereoisomer of **13**. D-*erythro*-Pentos-2-ulose (**15**, see Scheme 2) synthesized by oxidation of D-arabinose (**14**) according to Vuorinen et al.[42] was used as dicarbonyl source. The difference between L-*threo*-pentos-2-ulose (**12**, see Scheme 1) and **15** is the conformation of the stereogenic center at C-4, which may not affect the product spectrum. Compound **15** was allowed to react in $NaHCO_3$ buffer (pH 7.4) with N^{α}-*t*-Boc-L-lysine and N^{α}-*t*-Boc-L-arginine at 50 °C for 24 h (see Scheme 2). LC–(ESI)MS analysis prove formation of a signal with $[M+H]^+$ at m/z 633 (*t*-Boc-**16**). The protective groups were cleaved off in acidic medium (3 M HCl) and **16** with $[M+H]^+$ at m/z 433 was purified by preparative HPLC. Accurate mass determination of the isolated compound gave the expected elemental composition $C_{17}H_{33}N_6O_7$. The NMR data compiled in Table 1 proved the formation of N^6-[2-[(4-amino-4-carboxybutyl)amino]-5-[(1*S*,2*R*)-1,2,3-trihydroxypropyl]-3,5-dihydro-4*H*-imidazol-4-ylidene]-L-lysine (**16**) existing as a pair of diastereoisomers **16a** and **16b**. Isolation and structural characterization of **16a**,**b** indirectly proved the oxidative degradation of **5** via the intermediate L-*threo*-pentos-2-ulose (**12**) and the formation of **13** (see Scheme 1) as DHA **5** derived Maillard cross-link.

2.2. Structural assignment

Since compounds **9** and **11** (see Scheme 1), as well as **16** (see Scheme 2), represent novel lysine–arginine cross-links, special effort was invested in establishing their structures. All gs-HMBC spectra show only one single cross-peak for the H_2-1″ triplet in the downfield region, that is, with C-2. The other two cross-peaks connect this proton resonance with the non-hetero-substituted C-2″ and C-3″ of the arginine moiety. Alternative structures with endocyclic N^{δ} nitrogen of the L-arginine side chain, in contrast, would require correlation of H_2-1″ with both quasi-carbonyl carbons (C-2 and C-4) or with C-2 and C-5 in a five-membered ring.[36] The N^{δ} nitrogen of the L-arginine moiety thus the heterocyclic cores has remained exocyclic as provided by the analogous amino-imidazolinimine cross-link structures MODIC **1**, GODIC **2**, and DOGDIC **3**.[36]

For the novel lysine–arginine cross-links **9**, **11**, and **16**, ^1H and ^{13}C NMR chemical shifts (δ) and coupling constants (J) are compiled in Table 1. The arrows indicate significant carbon–proton long-range coupling across two or three bonds (^2J or ^3J). The NMR data sets for the heterocyclic core of **9**, **11**, and **16** are more or less consistent with those reported for MODIC **1** and GODIC **2**.[36] The characteristic carbon–proton long-range coupling connectivities from the gs-HMBC spectra prove the definite formation of the amino-imidazolinimine structures of **9**, **11**, and **16** (see Table 1). The postulated structure of **13** was indirect confirmed by the structural elucidation of the analogous compound **16**.

Threoses, highly reactive but not commonly occuring sugars have been shown to be significant participants in Maillard reactions involving DHA **5**. The reaction with lysine and arginine side chains leads to the formation of the amino-imidazolinium structures **9** and **11**.

Compound **12**, another oxidative degradation product of DHA **5**, represents the precursor dicarbonyl compound of the lysine–arginine cross-link **13**. Therefore, the influence of processing on food proteins as well as the significance in vivo will have to be examined in subsequent studies.

3. Experimental

3.1. General methods

^1H NMR (500 MHz), ^1H,^1H-COSY (correlation spectroscopy), ^1H,^1H-TOCSY (total correlation spectro-

scopy), gs-HSQC (gradient-selected heteronuclear single quantum coherence), and gs-HMBC (gradient-selected heteronuclear multiple bond correlation) spectra were recorded at 25 °C on a Varian (Darmstadt, Germany) Unity Inova 500 spectrometer in D_2O. The LC–(ESI, electrospray ionization)MS analyses were run on an HP1100 (Hewlett-Packard, Waldbronn, Germany) high-performance liquid chromatography (HPLC) system coupled to a Micromass (Manchester, U.K.) VG platform II quadrupole mass spectrometer equipped with an ESI interface. The HPLC system consists of an HP1100 autosampler, HP1100 gradient pump, HP1100 thermoregulator, and HP1100 diode array detector module. Column: 150 mm × 4.6 mm i.d., 5 μm, YMC-Pack Pro C 18; 10 mm × 4.6 mm i.d. guard column (YMC Europe, Schermbeck, Germany); column temperature, 25 °C; flow rate, 1.0 mL/min; injection volume, 20 μL. Gradients: 10 mM ammonium formate buffer (pH 4.0)–MeOH. (A) 5% MeOH, 0 min; 95% MeOH, 30–40 min; 5% MeOH, 45–50 min; 10 mM *n*-heptafluorobutyric acid (HFBA)-MeOH. (B) 5% MeOH, 0 min; 50% MeOH, 25 min; 95% MeOH, 30–35 min; 5% MeOH, 40–47 min. MS parameters: ESI^+ source temperature, 120 °C; capillary, 3.5 kV; HV lens, 0.5 kV; cone, 55 V. For LC analyses, the MS system was operated in the full scan mode (m/z 200–1000). For accurate mass determination, data were collected in the multichannel acquisition (MCA) mode with 128 channels per m/z unit using 12 scans (6 s) with 0.1 s reset time. The resolution was 1060–1110 (10% valley definition). The sample was dissolved in water/MeCN (1:1) containing reference material (0.1 μg/μL, see below), ammonium formate (0.1%), and formic acid (1%); the sample concentration was similar to that of the reference compound. The solution was introduced into the ESI source (80 °C) at a flow rate of 5 μL/min. The following scan ranges and reference peaks were used for calibration: **9**, m/z 360–490; poly(propylene glycol) 425, m/z 367.2696, 384.2971, 425.3108, 442.3391, 483.3538; **11**, m/z 360–465; poly(ethylene glycol) 400, m/z 371.2285, 388.2554, 415.2558, 432.2833, 459.2922; **16**, m/z 365–505; poly(propylene glycol) 425, m/z 367.2701, 384.2953, 425.3112, 442.3392, 483.3519, 500.3805. MassLynx 3.2 software was used for data acquisition and processing. The preparative HPLC system consisted of a Kronlab (Sinsheim, Germany) KD200/100SS gradient pump system combined with a Knauer (Berlin, Germany) A0293 variable wavelength detector and a 250 mm × 20 mm i.d., 7 μm, Nucleosil C 18 column with 50 mm × 20 mm i.d. guard column (Kronlab); injection volume, 1.5 mL; flow rate, 18 mL/min. Gradients were applied as follows: 10 mM ammonium formate buffer (pH 4.0)–MeOH. (A) 30% MeOH, 0 min; 70% MeOH, 15 min; 100%, 16–21 min; 30% MeOH, 24–30 min. (B) 0% MeOH, 0 min; 5% MeOH, 5–7 min; 0% MeOH, 8–13 min.

3.2. Materials

Milli-Q water, purified to 18 MΩ/cm^2 (Millipore, Eschborn, Germany), was used in the preparation of all solutions. HPLC grade MeOH was employed for LC and LC–MS. For preparative HPLC, solvents were degassed by flushing with helium. N^{α}-*t*-Boc-L-lysine, N^{α}-*t*-Boc-L-arginine, D-erythrose, and *n*-heptafluorobutyric acid (HFBA) were purchased from Fluka (Neu-Ulm, Germany); dehydroascorbic acid (DHA), poly(ethylene glycol) 400, and poly(propylene glycol) 425 were from Aldrich (Steinheim, Germany); diethylenetriaminepentaacetic acid (DTPA) was from Sigma (Steinheim, Germany). D-*erythro*-Pentos-2-ulose (**15**) was synthesized according to a procedure described previously.[42]

3.3. Synthesis of N^6-[2-[(4-amino-4-carboxybutyl)amino]-5-(2-hydroxyethyl)-3,5-dihydro-4*H*-imidazol-4-ylidene]-L-lysine (9) and N^6-[2-[(4-amino-4-carboxybutyl)amino]-5-(1,2-dihydroxyethyl)-3,5-dihydro-4*H*-imidazol-4-ylidene]-L-lysine (11)

Dehydroascorbic acid (**5**, 340 mg, 1.95 mmol), N^{α}-*t*-Boc-L-lysine (1.14 g, 4.15 mmol), N^{α}-*t*-Boc-L-arginine (1.52 g, 6.15 mmol), and diethylenetriaminepentaacetic acid (DTPA, 4 mg, 0.01 mmol) were dissolved in water (10 mL) and the pH was adjusted to 8 by adding solid $NaHCO_3$. The mixture was flushed with argon, kept at 37.4 °C for 7 days and purified by preparative HPLC (gradient A, detection wavelength, 244 nm). Fractions with retention time of 14.8 and 15.4 min yielded, after lyophilization, crude N^2-(*tert*-butoxycarbonyl)-N^6-[2-({4-[(*tert*-butoxycarbonyl)amino]-4-carboxybutyl}-amino)-5-(1,2-dihydroxyethyl)-3,5-dihydro-4*H*-imidazol-4-ylidene]-L-lysine (F I, *t*-Boc-**11**) and N^2-(*tert*-butoxycarbonyl)-N^6-[2-({4-[(*tert*-butoxycarbonyl)amino]-4-carboxybutyl}amino)-5-(2-hydroxyethyl)-3,5-dihydro-4*H*-imidazol-4-ylidene]-L-lysine (F II, *t*-Boc-**9**); LC–(ESI)MS (gradient A): F I, t_R 21.1 min, m/z 603 $[M+H]^+$; F II, t_R 21.6 min, m/z 587 $[M+H]^+$. Each fraction was dissolved in aqueous 3 M HCl (1.5 mL) and are kept at ambient temperature for 30 min. The pH was adjusted to 7 by slowly adding solid $NaHCO_3$, the volumes finally filled up to 5 mL and the mixtures were subjected to preparative HPLC (gradient B, detection wavelength, 244 nm). Fraction with t_R 6.4 min (F I) yielded, after lyophilization, **11** HCOOH (1 mg, 0.002 mmol, 0.12%) and fraction with t_R 9.7 min (F II) yielded, after lyophilization **9** HCOOH (2.9 mg, 0.007 mmol, 0.36%); UV (H_2O): λ_{max} (nm) (log ε) **11**, 242 (3.80), **9**, 242 (4.15); LC–(ESI)MS (gradient B): **11**, t_R 20.0 min, m/z 403 $[M+H]^+$; **9**, t_R 21.5 min, m/z 387 $[M+H]^+$. Accurate mass: **11** $[M+H]^+$ calcd for $C_{16}H_{31}N_6O_6$, 403.2305; found, 403.2323 ± 0.0006; **9** $[M+H]^+$ calcd for $C_{16}H_{31}N_6O_5$, 387.2356; found,

387.2350 ± 0.0012 (mean of nine measurements ± SD). For NMR data, see Table 1.

3.4. Formation of 9 and 11 by reaction of D-erythrose with N^{α}-*t*-Boc-L-lysine and N^{α}-*t*-Boc-L-arginine

D-Erythrose (23.4 mg, 0.2 mmol), N^{α}-*t*-Boc-L-lysine (152 mg, 0.62 mmol), and N^{α}-*t*-Boc-L-arginine (114 mg, 0.42 mmol) were dissolved in 1 mL of water and the pH was adjusted to 7.4 by slowly adding solid $NaHCO_3$. The reaction mixture was flushed with argon, kept at 50 °C for 24 h, aliquots were diluted 1:20 and subjected to LC–(ESI)MS analysis (gradient A, full scan mode): *t*-Boc-**11**, t_R 21.1 min, m/z 603 $[M+H]^+$; *t*-Boc-**9**, t_R 21.6 min, m/z 587 $[M+H]^+$.

3.5. Synthesis of N^6-[2-[(4-amino-4-carboxybutyl)amino]-5-[(1*S*,2*R*)-1,2,3-trihydroxypropyl]-3,5-dihydro-4*H*-imidazol-4-ylidene]-L-lysine (16)

N^{α}-*t*-Boc-L-lysine (1.82 g, 7.4 mmol), N^{α}-*t*-Boc-L-arginine (1.37 g, 4.98 mmol), and D-*erythro*-pentos-2-ulose (**15**, 500 mg, 2.3 mmol) were dissolved in water (12 mL) and the pH was adjusted to 7.4 by adding solid $NaHCO_3$. The mixture was flushed with argon, kept at 50 °C for 24 h and purified by preparative HPLC (gradient A, detection wavelength, 244 nm). Fractions with retention time of 14.3 min yielded, after lyophilization, crude N^2-(*tert*-butoxycarbonyl)-N^6-[2-({4-[(*tert*-butoxycarbonyl)amino]-4-carboxybutyl}amino)-5-[(1*S*,2*R*)-1,2,3-trihydroxypropyl]-3,5-dihydro-4*H*-imidazol-4-ylidene]-L-lysine (*t*-Boc-**16**, 20.8 mg, 0.033 mmol, 1.4%); LC–(ESI)MS (gradient A): t_R 21.1 min, m/z 633 $[M+H]^+$.

This crude product (20.8 mg, 0.033 mmol) was dissolved in aqueous 3 M HCl (3 mL) and kept at an ambient temperature for 30 min. The pH was adjusted to 7 by slowly adding solid $NaHCO_3$, the volume finally filled up to 5 mL, and the mixture subjected to preparative HPLC (gradient B, detection wavelength, 244 nm). Fractions with t_R 5.2 and 5.6 min yielded, after lyophilization, **16a** 2HCOOH (3.2 mg, 0.007 mmol, 18%) and **16b** 2HCOOH (1.5 mg, 0.003 mmol, 8.7%), respectively; UV (H_2O): λ_{max} (nm) (log ε) **16a**, 242 (4.13); LC–(ESI)MS (gradient B): **16a**, t_R 19.3 min, m/z 433 $[M+H]^+$; **16b**, t_R 19.5 min, m/z 433 $[M+H]^+$. Accurate mass: **16** $[M+H]^+$ calcd for $C_{17}H_{33}N_6O_7$, 433.2411; found, 433.2408 ± 0.0009 (mean of 11 measurements ± SD). For NMR data, see Table 1.

Acknowledgements

We are grateful to Dr. J. Conrad and S. Mika, Institute of Chemistry, University of Hohenheim, for the recording of the NMR spectra. We thank Dr. K. M. Biemel, CVUA Stuttgart, Fellbach, for many helpful discussions.

References

1. Ledl, F.; Schleicher, E. *Angew. Chem.* **1990**, *102*, 597–626.
2. Friedman, M. *J. Agric. Food Chem.* **1996**, *44*, 631–653.
3. Cheng, R.; Lin, B.; Lee, K.-W.; Ortwerth, B. *J. Biochim. Biophys. Acta* **2001**, *1537*, 14–26.
4. Sugimoto, H.; Shikata, K.; Wada, J.; Horiuchi, S.; Makino, H. *Diabetologia* **1999**, *42*, 878–886.
5. Chibber, R.; Molinatti, P. A.; Rosatto, N.; Lambourne, B.; Kohner, E. M. *Diabetologia* **1997**, *40*, 156–164.
6. Reiser, K. M. *Proc. Soc. Exp. Biol. Med.* **1998**, *218*, 23–37.
7. Nagaraj, R. H.; Sell, D. R.; Prabhakaram, M.; Ortwerth, B. J.; Monnier, V. M. *Proc. Natl. Acad. Sci. U.S.A.* **1991**, *88*, 10257–10261.
8. Biemel, K. M.; Bühler, H. P.; Reihl, O.; Lederer, M. O. *Nahrung/Food* **2001**, *3*, 210–214.
9. Kato, H.; Shin, D. B.; Hayase, F. *Agric. Biol. Chem.* **1987**, *51*, 2009–2011.
10. Brinkmann, E.; Wells-Knecht, K. J.; Thorpe, S. R.; Baynes, J. W. *J. Chem. Soc., Perkin Trans. 1* **1995**, 2817–2818.
11. Wells-Knecht, K. J.; Brinkmann, E.; Baynes, J. W. *J. Org. Chem.* **1995**, *60*, 6246–6247.
12. Wells-Knecht, K. J.; Zyzak, D. V.; Litchfield, J. E.; Thorpe, S. R.; Baynes, J. W. *Biochemistry* **1995**, *34*, 3702–3709.
13. Nissl, J.; Pischetsrieder, M.; Klein, E.; Severin, T. *Carbohydr. Res.* **1995**, *270*, C1–C5.
14. Glomb, M. A.; Monnier, V. M. *J. Biol. Chem.* **1995**, *270*, 10017–10026.
15. Vasan, S.; Zhang, X.; Kapurniotu, A.; Bernhagen, J.; Teichberg, S.; Basgen, J.; Wagle, D.; Shih, D.; Terlecky, I.; Bucala, R.; Cerami, A.; Egan, J.; Ulrich, P. *Nature* **1996**, *382*, 275–278.
16. Nagaraj, R. H.; Portero-Otin, M.; Monnier, V. M. *Arch. Biochem. Biophys.* **1996**, *325*, 152–158.
17. Buettner, U.; Gerum, F.; Severin, T. *Carbohydr. Res.* **1997**, *300*, 265–269.
18. Slatter, D. A.; Murray, M.; Bailey, A. J. *FEBS Lett.* **1998**, *421*, 180–184.
19. Lederer, M. O.; Gerum, F.; Severin, T. *Bioorg. Med. Chem.* **1998**, *6*, 993–1002.
20. Skovsted, I. C.; Christensen, M.; Breinholt, J.; Mortensen, S. B. *Cell. Mol. Biol.* **1998**, *44*, 1159–1163.
21. Sell, D. R.; Monnier, V. M. *J. Biol. Chem.* **1989**, *264*, 21597–21602.
22. Nagaraj, R. H.; Monnier, V. M. *Biochim. Biophys. Acta* **1992**, *1116*, 34–42.
23. Tessier, F.; Obrenovich, M.; Monnier, V. M. *J. Biol. Chem.* **1999**, *274*, 20796–20804.
24. Yamaguchi, M.; Nakamura, N.; Nakano, K.; Kitagawa, Y.; Shigeta, H.; Hasegawa, G.; Ienaga, K.; Nakamura, K.; Nakazawa, Y.; Fukui, I.; Obayashi, H.; Kondo, M. *Diabet. Med.* **1998**, *15*, 458–462.
25. Nagaraj, R. H.; Shipanova, I. N.; Faust, F. M. *J. Biol. Chem.* **1996**, *271*, 19338–19345.
26. Odani, H.; Shinzato, T.; Usami, J.; Matsumoto, Y.; Brinkmann-Frye, E.; Baynes, J. W.; Maeda, K. *FEBS Lett.* **1998**, *427*, 381–385.
27. Shamsi, F. A.; Nagaraj, R. H. *Curr. Eye Res.* **1999**, *19*, 276–284.
28. Ahmed, M. U.; Thorpe, S. R.; Baynes, J. W. *J. Biol. Chem.* **1986**, *261*, 4889–4894.
29. Biemel, K. M.; Friedl, D. A.; Lederer, M. O. *J. Biol. Chem.* **2002**, *277*, 24907–24915.

30. Lee, K.-W.; Mossine, V.; Ortwerth, B. J. *Exp. Eye Res.* **1998**, *67*, 95–104.
31. Argirov, O. K.; Lin, B.; Olesen, P.; Ortwerth, B. J. *Biochim. Biophys. Acta* **2003**, *1620*, 235–244.
32. Nagaraj, R. H.; Monnier, V. M. *Biochim. Biophys. Acta* **1995**, *1253*, 75–84.
33. Simpson, G. L. W.; Ortwerth, B. J. *Biochim. Biophys. Acta* **2000**, *1501*, 12–24.
34. Shin, D. B.; Feather, M. S. *Carbohydr. Res.* **1990**, *208*, 246–250.
35. Biemel, K. M.; Reihl, O.; Conrad, J.; Lederer, M. O. *J. Biol. Chem.* **2001**, *276*, 23405–23412.
36. Lederer, M. O.; Klaiber, R. G. *Bioorg. Med. Chem.* **1999**, *7*, 2499–2507.
37. Konishi, Y.; Hayase, F.; Kato, H. *Biosci. Biotechnol. Biochem.* **1994**, *58*, 1953–1955.
38. Hayase, F.; Koyama, T.; Konishi, Y. *J. Agric. Food Chem.* **1997**, *45*, 1137–1143.
39. Henle, T.; Walter, A. W.; Haessner, R.; Klostermeyer, H. *Z. Lebensm. Unters. Forsch.* **1994**, *199*, 55–58.
40. Lo, T. W. C.; Westwood, M. E.; McLellan, A. C.; Selwood, T.; Thornalley, P. J. *J. Biol. Chem.* **1994**, *269*, 32299–32305.
41. Nishikawa, Y.; Toyoshima, Y.; Kurata, T. *Biosci. Biotechnol. Biochem.* **2001**, *65*, 1707–1712.
42. Vuorinen, T.; Serianni, A. S. *Carbohydr. Res.* **1990**, *207*, 185–210.